Microscopic interaction effects of prestressed geogrids in a reinforced soil element

C. Lackner
STRABAG AG, Central Technical Head Office, Division Geotechnical Engineering, Wien, Austria,
D.T. Bergado
Asian Institute of Technology, School of engineering and Technology, Bangkok, Thailand
S. Semprich & R. Marte
Graz University of Technology, Institute of Soil Mechanics and Foundation Engineering, Graz, Austria

ABSTRACT: In this paper, investigations on prestressed geogrids in reinforced soil element tests utilizing Discrete Element Method (DEM) modeling are presented. A microscopic three dimensional (3D) Discrete Element model is constituted to evaluate displacements and contact forces between discrete gravelly particles in a prestressed reinforced soil element. The granular soil particles and the discrete geogrid reinforcement were numerically modeled by "Computer Aided Design" (CAD). The load transfer mechanism between the soil particles and the geogrid reinforcement was evaluated. Arching effects occurred randomly between the granular soil particles and the discrete longitudinal and transverse members of the geogrid. These arching effects lead to local force concentrations between the generated particles and to high tensile forces in the numerically bonded geogrid. In addition, three soil geogrid interaction effects were determined. In the case of discrete clumps entering the gaps of the discrete geogrid, the longitudinal and transverse members of the reinforcement were expanded. This effect had already been classified as static or dynamic interlocking effect in literature. While loading the reinforced soil element, grains also entered between the single strings of the longitudinal and transverse members of the woven geogrid reinforcement. This effect was newly defined as single string interaction effect. In longitudinal but also in transverse direction the geogrid aligned to the surrounding granular particles. This newly defined alignment effect led to a permanent contact between geogrid and soil particles and thereby resulted in a permanent interfriction effect. The provided numerical model gave a realistic and detailed insight in the fundamental load transfer and soil geogrid interaction behavior in case of utilizing the concept of prestressed reinforced soil.

Keywords: Prestressed reinforced soil, geogrid, discrete element, clump, microscopic

1 INTRODUCTION

The discrete soil geogrid interaction has been investigated by several researchers in the last years. Three dimensional discrete element simulations have been utilized to model numerical triaxial tests on soil elements reinforced with one to three layers of a geometrically detailed modelled geogrid.

Konietzky et al. (2004) conclude that the performed DEM simulations of triaxial reinforced soil element tests have given a valuable insight into the soil geogrid interaction mechanism. Discrete Element Method (DEM) simulations have been used to model the interaction between ballast material and a geogrid by simulating pull-out tests and comparing their results with experimental data by McDowel et al. (2006). The DEM simulations predict precisely the peak mobilized resistance and the displacement necessary to mobilise a peak pull-out force. In addition, the effect of the ratio of the geogrid aperture size to ballast particle diameter on the pull-out resistance has been investigated. McDowel et al. (2006) found that a value of 1.4 is the ideal ratio between the opening size of the geogrid and the diameter of the grain.

Zhang et al. (2007) performed discrete simulations of pullout tests to investigate the effect of compaction of the reinforced soil body on the pullout force during the tests. The results of the discrete modelling have correlated with the tests results gained from laboratory studies.

Bhandari & Han (2010) have utilized two dimensional Discrete Element modelling to investigate the soil geotextile interaction under a cyclic vertical load. The DEM results show that the geotextile prevents the particles from vertical movement. Bhandari & Han (2010) state that the benefit of the geotextile in minimizing the vertical deformation depends on the vertical position of the geotextile.

Tutumluer et al. (2009) conducted a detailed discrete element study on direct shear tests including two different shapes (angular and triangular) of discrete geogrids. Out of the utilized numerical simulations but also as a result of conducted direct shear tests in the laboratory. Tutumluer et al. (2009) found out that the soil geogrid interaction coefficients becomes higher than 1.0 in case of reinforcing the soil element in the shear box. This is due to the interlocking effects between the discrete particles and the gaps of the geogrid reinforcement.

2 OVERVIEW ON THE NUMERICAL MODEL

A three dimensional Discrete Element model has been utilized to investigate the mesoscopic load transfer and soil geogrid interaction mechanism of a prestressed geogrid in a soil element. The three dimensional Discrete Element Method code, “Particle Flow Code (PFC^{3D}), Version 4.00-191 64-bit”, has been employed (Itasca Consulting Group 2005). A cubical model (edge length = 0.1 m) with geometrically detailed modelled grains and geogrid has been set up. The granular soil particles and the discrete geogrid reinforcement have been modelled “Computer Aided Design” (CAD). The granular soil particles have been mesoscopically investigated in detail and generated as clumps in PFC^{3D} (Itasca Consulting Group 2005).

3 NUMERICAL SETUP AND CALCULATION PROCESS

The Itasca Consulting Group (2005) provides the fundamental principles on Discrete Element modelling with the Particle Flow Code in three dimensions (PFC^{3D}). Fundamentals have been prepared by Halsegger (2004), Zöhrer (2006) and Lenzi (2009).

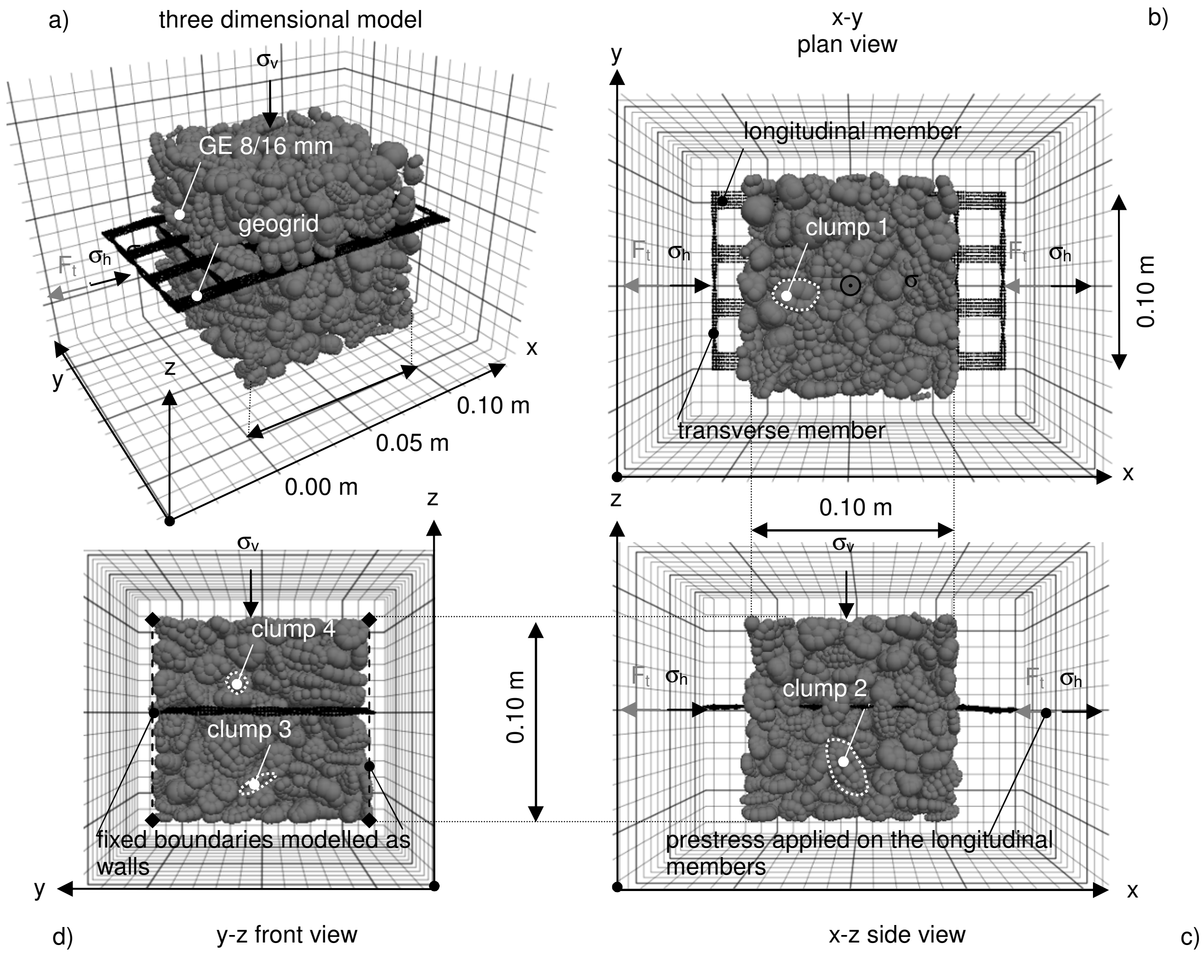

Figure 1: Schematic sketch of the overview on the Discrete Element model: a) three dimensional model including boundary fixities b) x-y plan view c) x-z side view d) y-z front view.

The basic geometry information of the numerical model is presented in Figure 1. The three dimensional model (Fig. 1a) is generated by utilizing CAD designed clumps, representing the granular soil particles and a CAD designed discrete geogrid reinforcement.

Figure 1b) represents the x-y plan view of the model. The longitudinal and transverse members of the geogrid and the shape of clump 1 are schematically shown. Additionally the applied stress boundaries σ_v and σ_h according are presented. The tensile force F_t of the geogrid reinforcement is shown in Figure 1b).

Figure 1c) shows the x-z side view of the numerical model. An additional prestress is applied to the longitudinal members of the discrete geogrid in case of utilizing the concept of PRS_i.

The fixed boundaries of the model are shown in Figure 1d). The boundary conditions are numerically modelled by so called wall elements (Itasca Consulting Group 2005). The calculated stresses have been applied by programming servo controlled walls. Thereafter, velocities are applied on the wall. The velocities result in a movement of the walls. Due to the contact forces between the particles, the walls obtain stresses depending on the movement of the wall. The walls stop, when the stresses have reached the calculated input value according to a performed multiscale FEM analysis (Lackner et al. 2012).

4 NUMERICAL MATERIAL PARAMETERS

The mesoscopic investigated gravelly material (Lackner et al. 2012) has been numerically modelled in detail. The shape of the grains has been modelled by so called clumps (Itasca Consulting Group 2005). These clumps have been implemented in the numerical model as described in Figure 2.

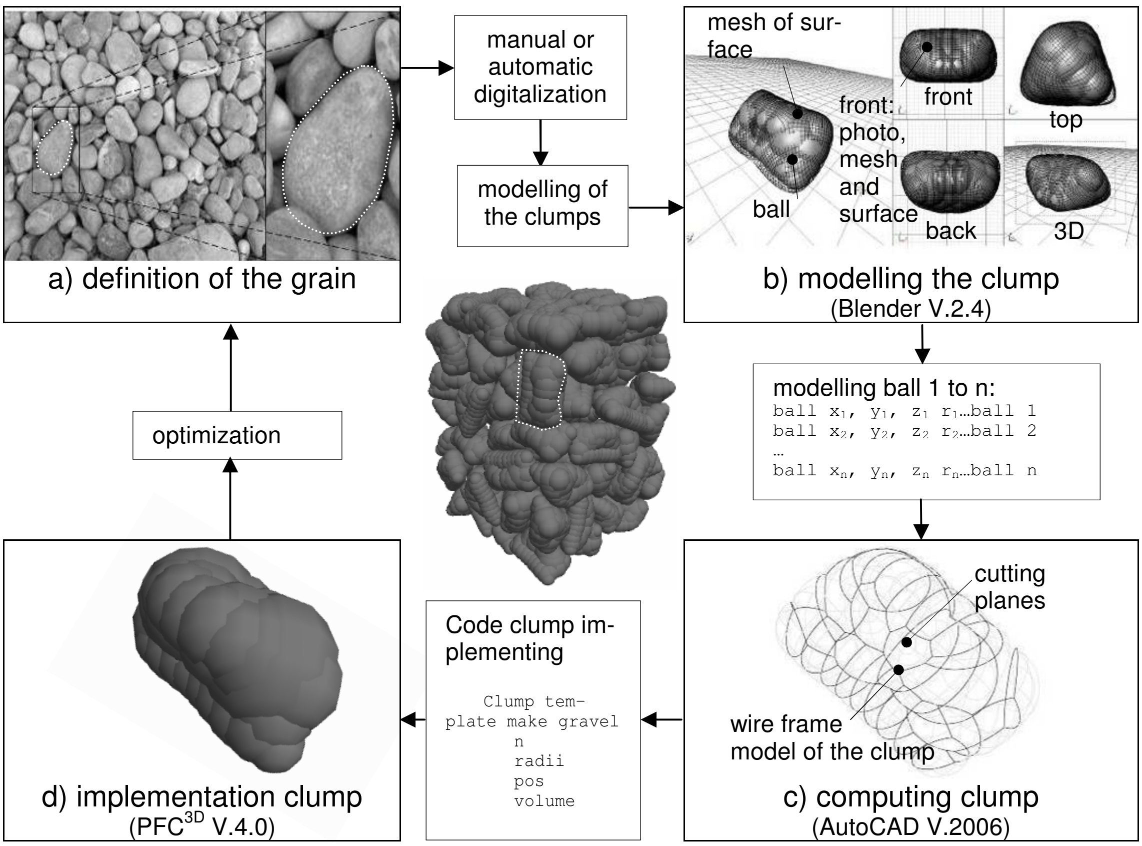

Figure 2: Schematic sketch of a generation, digitalization and implementation process of a discrete clump: a) definition of the grain b) modelling of the clumps surface and filling with spheres c) computing the clumps volume d) implementation of the clump in the DEM model code.

The surface of a predefined grain has been modelled by utilizing the software Blender (Version 2.4). The shape of the grain is first visualized by implementing 3 photos of the grain with different perspectives into the software Blender. The surface of one clump is then modelled by generating a mesh representing the surface of the grain (Fig. 2b). The generated mesh is refined until the virtual and real surfaces correlate well. The surface of the clump is modelled accurately. Once the surface is generated the volume inside the surface is filled with spheres. Finally a clump is generated and imported into the DEM model.

The density of the granular material has been measured in the laboratory (Lackner et al. 2012) and amounts to 2.64 g/cm³. The Hertz Mindlin model (Itasca Consulting Group 2005), an appropriate contact model for modelling granular particle interaction, has been implemented into the numerical simulation. The input stiffness parameters for this contact model are given in Table 1. These values results from back analyzed large scale oedometer tests and correlates well with the values from literature as reported by Scharinger (2007).

Table 1: DEM soil parameters for granular backfill material

parameter	PFC	unit	value
density	*density*	[kg/m³]	2.64E+03
shear modulus	*shear*	[N]	3.00E+10
Poisson's ratio	*poiss*	[-]	0.2
normal stiffness	k_n	[N/m]	3.90E+06
shear stiffness	k_s	[N/m]	9.00E+05
friction coefficient	*friction*	[-]	0.8
local damping	*damp local*	[-]	0.90/0.00
viscous damping (normal/shear)	*damp viscous*	[-]	0.00/0.97

The local and viscous damping parameters are attached to Table 1. Local damping *damp local* is set to a value of 0.90 to accelerate quasi static analyses such as loading processes. No viscous damping is activated (damp viscous = 0.00). In the case of modelling a filling process or when dumping and dropping soil particles the viscous damping coefficient *damp viscous* is set to a value of 0.97.

Table 2: DEM material parameters for woven, biaxial, PET geogrid (according to Dijak 2012)

parameter geogrid	PFC	unit	value	
			detailed	standard
density	*density*	[kg/m³]	1.03E+03	2.06E+03
normal stiffness	k_n	[N/m]	4.00E+06	1.3E+07
shear stiffness	k_s	[N/m]	8.50E+05	6.00E+04
contact bond normal strength	*n_bond*	[N]	5.00E+05	5.00E+05
contact bond shear strength	*s_bond*	[N]	5.00E+05	5.00E+05
radius multiplier	*pb_radius*	[-]	0.29	0.15
parallel bond normal stiffness	pb_k_n	[Pa/m]	2.80E+12	1.25E+13
parallel bond shear stiffness	pb_k_s	[Pa/m]	1.80E+12	3.00E+11
parallel bond normal strength	$pb\_n_{strength}$	[Pa]	8.00E+14	8.00E+14
parallel bond shear strength	$pb\_s_{strength}$	[Pa]	8.00E+14	8.00E+14
friction coefficient	*friction*	[-]	0.5	0.5

If a clump interacts with a sphere representing the geogrid reinforcement, a linear elastic contact is assumed. The normal and shear stiffness ratios k_n and k_s are given in Table 1. In order to model interfriction processes, a microscopic roughness $\mu = 0.8$ is applied to the Hertz Mindlin slip model. The shear properties have been calibrated by performed large scale direct shear tests.

The shape of the geogrid has been designed computer aided. The longitudinal and transverse members of the reinforcement material have been modelled in detail by bonding single spheres to each other. Additionally a standard geogrid has been modelled. The members of the geogrid consist of single spheres bonded together next to each other. The material properties have been estimated by calibrating the standard and detailed geogrid with conducted laboratory tests (Dijak 2012). Table 2 provides the numerical microscopic parameters of the geogrid. The geogrid is modelled with a linear elastic soft-contact model. The density of the single spheres has been estimated by numerically back-modelling a weighing machine where a geogrid with an area of 0.1 * 0.1 m² is placed.

The experimental and numerical results coincide when the detailed geogrid is generated by spheres with a density of 1.03 g/cm³. The tensile strength and stiffness properties of the detailed geogrid are calibrated by (Lackner et al. 2012) performing tensile strength tests and back analyzing the experimental procedure. The experimentally and numerically investigated tensile stress-strain curves agree when the normal stiffness k_n of the numerical geogrid amounts to 4.00E+06 N/m. The shear stiffness of the reinforcement has been fixed to a value of k_s = 8.50E+05 N/m. The contact bond`s normal and shear strength *n_bond* respectively *s_bond* have been set to a value of 5.00E+05 N.

The flexural behaviour of the geogrid is calibrated by back analysing performed bending tests with the geogrid. The parallel bond normal and shear stiffness pb_k_n and pb_k_s describe the bending deformation behaviour of the material (Itasca Consulting Group, 2005). The parallel bond`s normal stiffness pb_k_n has finally been fixed to a value of 2.80E+12 Pa/m. The parallel bond shear stiffness pb_k_s amounts to 1.80E+12 Pa/m. These values linearly correlate with the predefined radius multiplier *pb_radius*. The radius multiplier is set to 29 % of the value of the mean radius of two spheres bonded together.

The normal and shear strength parameters $pb\_n_{strenght}$ respectively $pb\_s_{strength}$ are finally set to a value of 8.00E+14 Pa. These parameters define the strength properties of the parallel bond (Itasca Consulting Group 2005). The friction coefficient *friction* is finally calibrated by performing large scale direct shear tests (Dijak 2012). A friction coefficient of 0.5 has been back analyzed.

5 NUMERICAL RESULTS AND DISCUSSION

Figure 3 shows the DEM model of the reinforced (RE) soil element to evaluate the mesoscopic load transfer mechanism. Figure 3a) presents the side view (y-z) of the soil element.

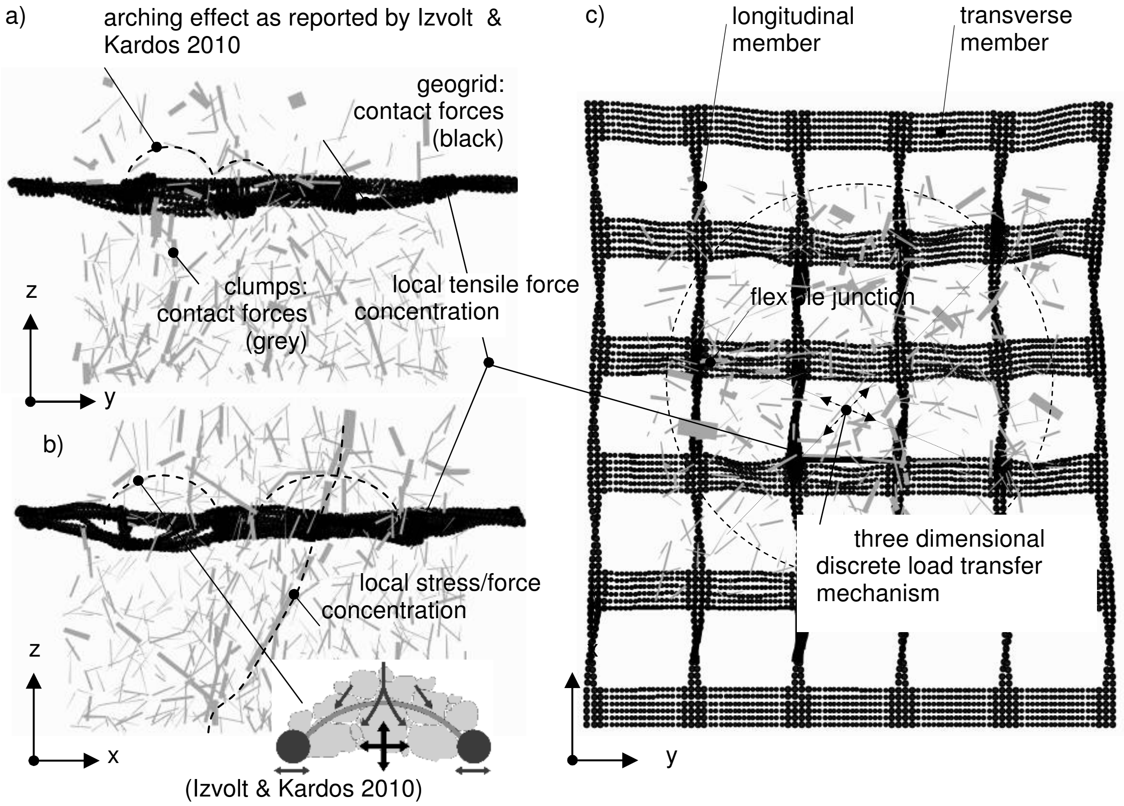

mesoscopic information
soil: 443 clumps _18 spheres_9 contacts/clump_2 active contacts geogrid: 4333 spheres_5046 bonds

Figure 3: DEM mesoscopic modelling of reinforced (RE) soil element to evaluate the mesoscopic load transfer mechanism: a) side view (y-z) including contact forces between the granular particles and tensile force distribution along geogrid b) front view (x-z) including contact forces between the granular particles and tensile force distribution along geogrid c) plan view (x-y) including contact forces between the granular particles and tensile force distribution along geogrid.

The results include the contact forces (grey) between the granular particles and tensile force distribution (black) along the geogrid. Arching effects, as reported by Izvolt & Kardos in 2010, occur randomly between the granular soil particles and the discrete geogrid. Those arching effects lead to local stress concentrations between the particles and to high tensile forces in the geogrid at certain places. This effect is also visible in the front view (x-z) of the reinforced soil element (Fig. 3d).

Figure 3c) presents the plan view of the soil element. The contact forces (grey) between the clumps are plotted additionally. It is shown that the load is transferred randomly in three dimensions. The discrete mechanism may be assumed to act in two main directions. These directions are inclined with regard to the longitudinal and transverse members of the geogrid. The inclination of the load transfer direction mainly depends on the particles, their shape and their location. Figure 3 additionally contains the mesoscopic contact information of the soil and geogrid particles included in the reinforced soil element.

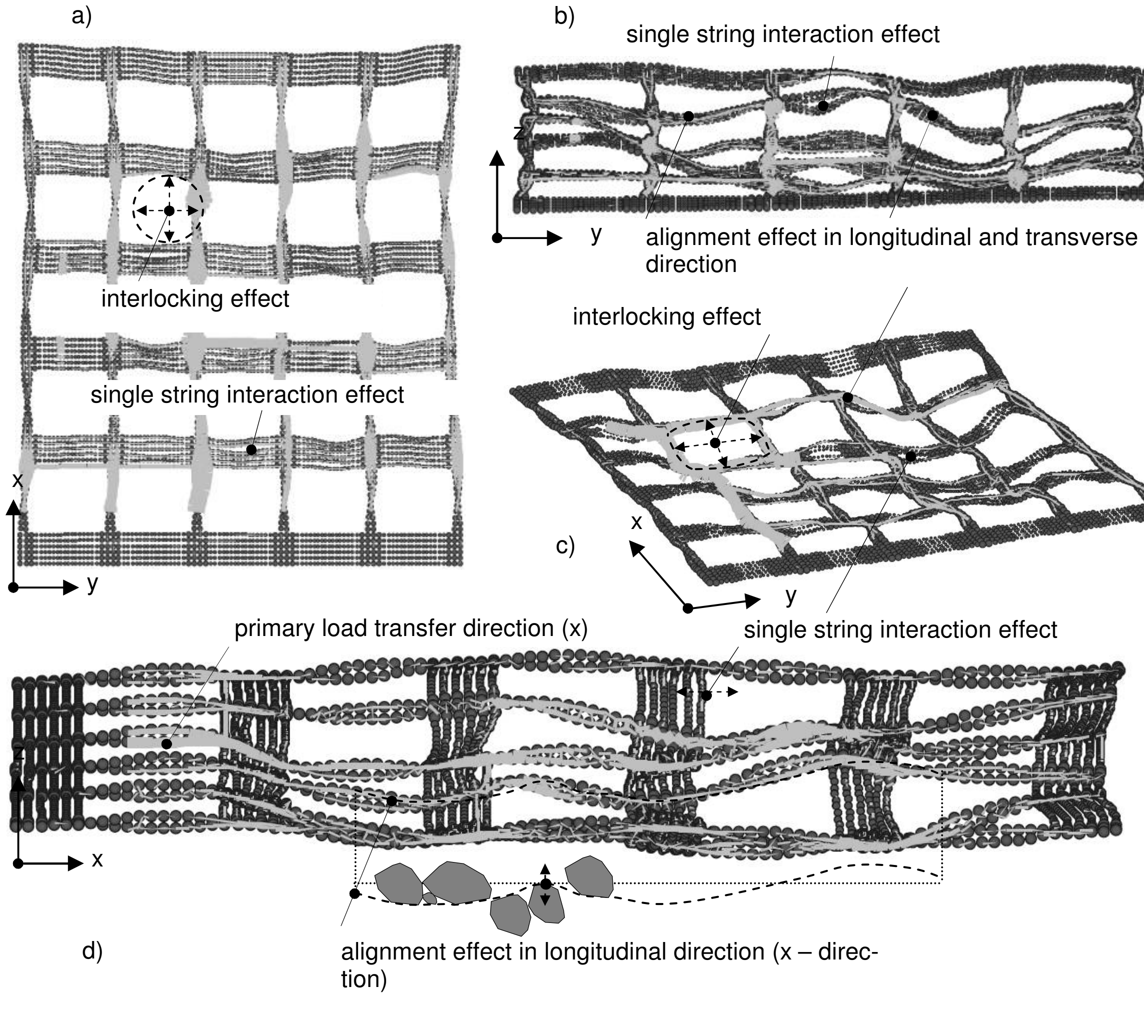

Figure 4: DEM mesoscopic modelling of reinforced (RE) soil element to evaluate the mesoscopic deformation of the geogrid reinforcement: a) plan view (x-y) of the geogrid including tensile force distribution along geogrid and interlocking effect b) side view (y-z) including tensile force distribution along geogrid and single string interaction effect c) 3D view (x-y) including tensile force distribution along geogrid d) front view (x-z) including tensile force distribution along geogrid and alignment effect.

Figure 4 shows the mesoscopic DEM model of the reinforced (RE) soil element to evaluate the mesoscopic deformation of the geogrid reinforcement. Three different soil geogrid interaction effects have been determined by analysing the discrete deformation behaviour of the reinforcement under loading.

Figure 4a) presents the plan view of the deformed geogrid. The tensile forces (grey) of the geogrid are plotted additionally. When the discrete clumps enter the gaps of the discrete geogrid, the longitudinal and transverse members of the reinforcement are pushed sideward. This effect is called interlocking effect (Fig. 4a). Figure 4b) shows the side view (y-z) of the reinforced soil element. While loading the soil element, clumps get in between the single strings of the longitudinal and transverse members of the reinforcement. This effect is defined as single string interaction effect. These two effects, interlocking and single string interaction, are well visible in the case of plotting the geogrid in three dimensions (Fig. 4c).

The front view (x-z) of the element test and the tensile force distribution along the longitudinal and transverse members of the geogrid are shown in Figure 4d). In the longitudinal and in the transverse direction the geogrid aligns to the surrounding granular particles. This so called alignment effect results in a permanent contact between geogrid and soil particles. The more contact, the more friction can be transferred from the soil particles to the geogrid and other way round.

In case of utilizing the concept of PRS_i it is visible that the geogrid does not highly align around the particles in the longitudinal direction. This is again due to the prestress in the reinforcement. As shown in Lackner 2012 this may results in gaps between the reinforcement and the surrounding particles. Further, this results in lower interfriction between soil and reinforcement. Although positive interaction effects such as the alignment effect, may be reduced, the concept of prestressed reinforced soil results in an improvement of the soil structure.

The mesoscopic analyses show the load transfer mechanism between soil and reinforcement in detail. Three effects have been observed and defined. They mesoscopically explain the positive consequences when utilizing the concept of PRS_i. As a final conclusion it can be stated that the soil geogrid interaction can be simulated well by utilizing the innovative concept of CAD clumps and geogrids for DEM simulations.

6 SUMMARY AND CONCLUSIONS

A mesoscopic DEM analysis has been performed. In order to present reliable results, a detailed DEM microscopic calibration has been conducted. Once the microscopic numerical parameters are fixed, three dimensional discrete and differently reinforced soil elements have been modelled. The soil elements represent the mesoscopic interaction behaviour between the reinforcement and the surrounding soil structure.

The mesoscopic load transfer mechanism of the reinforced (RE) soil element has been evaluated. Arching effects as reported by Izvolt and Kardos in 2010 have occurred randomly between the granular soil particles and the discrete geogrid. Those arching effects have led to local stress concentrations between the particles and to high tensile forces in the geogrid at certain places.

Moreover, three different soil geogrid interaction effects have been determined. When the discrete clumps have entered the gaps of the discrete geogrid, the longitudinal and transverse members of the reinforcement have been pushed sidewards. This effect has been classified as interlocking effect. While loading the soil element, clumps have entered between the single strings of the longitudinal and transverse members of the reinforcement. This effect has been defined as single string interaction effect. In longitudinal but also in transverse direction the geogrid has aligned to the surrounding granular particles. This so called alignment effect has resulted in a permanent contact between geogrid and soil particles.

The deformation behaviour of the reinforced soil element has been observed in case of utilizing the concepts of PRS_i. Displacements above the geogrid layer have been higher than below the geogrid. The results have shown a sound agreement with respect to the results gained from FEM and PIV analyses . So called arching effects have become visible. These effects have resulted, in local stress concentrations between the soil particles. The tensile force of the geogrid has distributed constantly along the reinforcement in longitudinal direction. This has been due to the permanent prestress in the longitudinal direction. In the case of utilizing the concept of PRS_i, the transverse members have been strained in the longitudinal direction. The discrete clumps have accessed between the single strings. The geogrid has not aligned around the particles in the longitudinal direction. This has mainly been due to the prestress in the reinforcement. This may result in gaps between the reinforcement and the surrounding particles.

The final conclusion is that the system of PRS_i has been numerically validated. As reported by Lackner in 2012 it may be concluded that by using the same materials, soil and reinforcement and by prestressing the geogrid reinforcement with the presented concept the load displacement behaviour of reinforced soil structures can be increased steadily.

REFERENCES

Bhandari, A.; Han, J. (2010). Investigation of geotextile-soil interaction under a cyclic vertical load using the discrete element method. Geotextiles and Geomembranes, Vol. 28, 33-43.

Dijak, M. (2012). Dreidimensionale numerische Modellierung von Laborversuchen mit Geokunststoffen unter Verwendung der Diskreten Elemente Methode. Master thesis, Graz University of Technology, Institute of Soil Mechanics and Foundation Engineering (in German).

Halsegger, W. (2004). Experimentelle und numerische Untersuchungen zur geführten Senkkastenbauweise unter besonderer Berücksichtigung des Eindringvorganges d er Schneide und der Risiken des Verfahrens. PhD thesis, Graz University of Technology, Gruppe Geotechnik Graz, No. 23 (in German).

Itasca Consulting Group (2005). Particle Flow Code in 3 Dimensions. Itasca Consulting Group, Inc., Minneapolis.

Izvolt, L.; Kardos, J. (2010). Parameter von Geogittern und ihr Einfluss auf deren Wirksamkeit im Eisenbahnunterbau. ETR Eisenbahntechnische Rundschau, No.4, 176-186 (in German).

Konietzky, H.; te Kamp, L.; Jenner, C. (2004). Use of DEM to model the interlocking effect of geogrids under static and cyclic loading. Numerical Modeling in Micromechanics via Particle Methods, A.A. Balkema, 3-11.

Lackner, C. (2012). Prestressed reinforced soil – Concept, investigations and recommendations. PhD thesis, Graz University of Technology, Gruppe Geotechnik Graz, No. 45.

Lackner, C.; Bergado, D.T.; Semprich S. (2012). Prestressed reinforced soil by geogrids - Theory, experimental and numerical investigations. Proceedings of the Geoamericas 2012 Conference (CD – Rom).

Lenzi, M. (2009). Untersuchungen von mit Pfählen gesicherten Rutschhängen mit der Diskreten Elementemethode. PhD thesis, Graz University of Technology, Gruppe Geotechnik Graz, No. 37 (in German).

McDowell, G.R.; Herireche, O.; Konietzky, H.; Brown, S.F. (2006). Discrete element modelling of geogrids-reinforced aggregates. Geotechnical Engineering – ICE 159 (GE1), 35-48.

Scharinger, F. (2007). A Multilaminate Model for Soil incorporating Small Strain Stiffness. PhD thesis, Graz University of Technology, Gruppe Geotechnik Graz, No. 31.

Tutumluer, E.; Huang, H.; Bian, X. (2009). Research on the behaviour of geogrids in stabilisation applications. Jubilee Symposium on Polymer Geogrid Reinforcement, London (unpublished).Zhang, J.; Yasufuku, N.; Ochiai, H. (2007). A few considerations of pullout test characteristics of geogrid reinforced sand using DEM analysis. Geosynthetics Engineering Journal, 22, 103-110.

Zöhrer, A. (2006). Laboratory Experiments and Numerical Modelling of Cone Penetration Tests into various Martian Soil Analoque Materials. PhD thesis, Graz University of Technology, Gruppe Geotechnik Graz, No. 29.